

# Estimation of rotor position of a sensorless doubly fed induction generator

**Ranjay Das**

Assistant Professor, Electrical Engineering Department,  
Central Institute of Technology Kokrajhar, BTR Assam, India 783370  
r.das@cit.ac.in

**Abstract:** Widespread installation of Distributed Generation (DG) in power system network creates a new area of research for finding the improvement of power system network. Doubly Fed Induction Generator (DFIG) run by wind turbine can be worked as a DG. DFIG can supply active power to the network. Systems voltage profile improves while DFIG generates the active power. DFIG rotor is coupled with wind turbine and stator side is directly connected to the constant frequency three phase grid. Wind speed varies throughout the day that is why asynchronous machine is used to harness wind energy. Wind energy is converted to electrical energy. DFIG supplies the active power to the distribution system. Algorithm for estimation of rotor position and speed is presented in this paper. Details of the algorithms and relevant simulation results are present ed.

**Keywords:** Distributed Generation, Doubly Fed Induction Generator, Active Power, Reactive Power

(Article history: Received: 2<sup>nd</sup> February 2021 and accepted 25th June 2021)

## I. INTRODUCTION

Distributed Generations (DGs) are mainly run by different types of renewable energy sources. Among these energy sources, wind energy is most promising. Wind velocity changes throughout the day. As a consequence, wind power plant needs variable speed generator to improve the aerodynamic efficiency of the rotor. That is why asynchronous generators (mainly induction generators) are used as DG to tap the wind energy. There are two types of induction generators-Squirrel Cage Induction Generator (SCIG) and Doubly Fed Induction Generator (DFIG). SCIG and DFIG represents an interesting solution for the application of wind power generation [1]–[3]. SCIG is singly excited machine and DFIG is doubly excited machine. Rotor side of the DFIG is accessible and can be connected with external power supply. Wind-driven SCIG-based DG can be integrated with radial distribution system [1].

DFIG stator is directly connected to the constant frequency three-phase grid and the rotor is supplied by back-to-back PWM voltage-source converters. This configuration is suitable in wind-power generation [4], [5]. DFIG supplies active as well as reactive power. Decoupled control of active and reactive powers is possible using DFIG [4]. Voltage stability of the power system network is improved by the reactive power generation of the DFIG [6].

Various types of control for DFIG have been proposed in the literature. These are controlling the electromagnetic torque, controlling the rotating speed, controlling the stator active power, and optimisation technique to search for the optimal parameters of controllers [7], [8]. Proportional-Integral controllers are well accepted and highly used for reliability and robustness. Suitable parameters are needed for controllers to achieve better control performance. Genetic algorithm is used to tune the controller parameter [8].

Likewise, direct power control scheme can be applied to achieve nonoscillating torque accompanied by the removal of non-sinusoidal current exchange with the grid [9].

In every control, speed and rotor position measurement is required. Encoder is required to measure the speed and rotor position. Without connecting the encoder, estimation of the speed and rotor position is possible. In this paper, position and speed of rotor of DFIG are estimated and compared with the encoder. Algorithm for estimation is given. Algorithm is developed from the basic equations of the induction machines. Three phase winding to two phase winding conversion of induction machine is done to get the algorithm. Simulation work is done in PSCAD software.

## II. PROBLEM FORMULATION

Figure 1 shows the equivalent circuit of an induction machine. Voltage  $\underline{u}_s$  is applied across stator side. Rotor side is supplying current  $\underline{i}_r$  referred to stator.

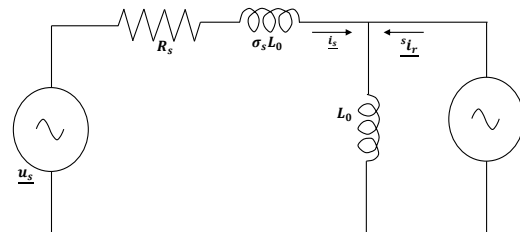


Fig. 1. Equivalent circuit referred to stator

Magnetizing inductance is  $L_0$ , resistance of the stator phase winding is  $R_s$ , Leakage factors of the stator phase winding is  $\sigma_s$ .

Stator side voltage equation is

$$\underline{u}_s = R_s \underline{i}_s + (1 + \sigma_s) L_0 \frac{d}{dt} \underline{i}_s + L_0 \frac{d}{dt} \underline{i}_r e^{j\epsilon} \quad (1)$$

$$\underline{u}_s = R_s \underline{i}_s + L_0 \frac{d}{dt} [(1 + \sigma_s) \underline{i}_s + \underline{i}_r e^{j\epsilon}] \quad (2)$$

The magnetizing current vector is defined as

$$\underline{i}_{ms} = (1 + \sigma_s) \underline{i}_s + \underline{i}_r e^{j\epsilon} \quad (3)$$

$\underline{i}_{ms}$  is the equivalent current vector in the stator reference frame responsible for producing the stator flux  $\underline{\psi}_s$ .

$$\underline{u}_s = R_s \underline{i}_s + L_0 \frac{d}{dt} \underline{i}_{ms} \quad (4)$$

Stator resistance  $R_s$  is very small, so it is neglected. In that case,  $\underline{i}_{ms}$  is lagging  $\underline{u}_s$  by  $\pi/2$ . This is shown in Fig. 3.  $\underline{u}_s$  is along the q-axis and  $\underline{i}_{ms}$  is along the d-axis.

### A. Computation of $\sin\theta$ and $\cos\theta$

$\underline{u}_s$  is making angle  $\theta$  with the stator axis as shown in Fig. 3. Induction machine has symmetrical three phase coil systems both on the stator and the rotor, which can be represented by two equivalent two-phase coil systems as shown in Fig. 2. From Fig. 2, it is clear that the rotor axis makes an angle  $\epsilon(t)$  with respect to the stator axis. The rotor current space phasor in stator reference frame can be written as:

$$\underline{i}_r(t) = i_{s\alpha}(t) + j i_{s\beta}(t) \quad (5)$$

$\alpha$  and  $\beta$  components of stator current can be written as:

$$i_{s\alpha}(t) = \frac{3}{2} i_{s1}(t) \quad (6)$$

$$i_{s\beta}(t) = \frac{\sqrt{3}}{2} (i_{s2}(t) - i_{s3}(t)) \quad (7)$$

The rotor current space phasor in rotor reference frame can be written as:

$$\underline{i}_r(t) = i_{ra}(t) + j i_{rb}(t) \quad (8)$$

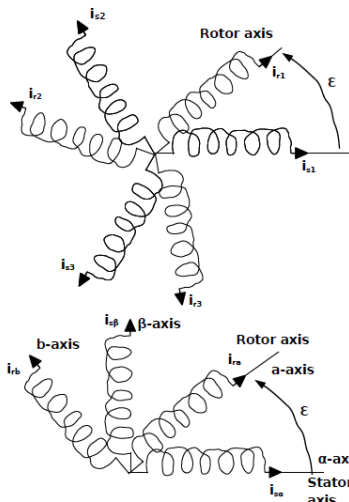


Fig.2. Three-phase and equivalent two-phase winding

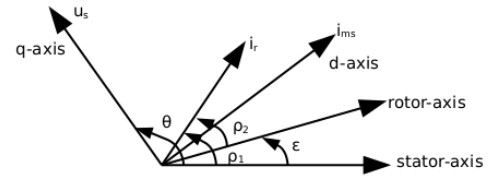


Fig. 3. Phasor diagram

$a$  and  $b$  components of stator current can be written as:

$$i_{ra}(t) = \frac{3}{2} i_{r1}(t) \quad (9)$$

$$i_{rb}(t) = \frac{\sqrt{3}}{2} (i_{r2}(t) - i_{r3}(t)) \quad (10)$$

Similarly, the stator voltage space phasor in stator reference frame can be written as:

$$\underline{u}_s(t) = u_{s\alpha}(t) + j u_{s\beta}(t) \quad (11)$$

$\alpha$  and  $\beta$  components of stator current can be written as:

$$u_{s\alpha}(t) = \frac{3}{2} u_{s1}(t) \quad (12)$$

$$u_{s\beta}(t) = \frac{\sqrt{3}}{2} (u_{s2}(t) - u_{s3}(t)) \quad (13)$$

Magnitude of stator voltage space phasor is

$$|\underline{u}_s(t)| = \sqrt{u_{s\alpha}(t)^2 + u_{s\beta}(t)^2} \quad (14)$$

$$\sin\theta = \frac{u_{s\beta}(t)}{|\underline{u}_s(t)|} \quad (15)$$

$$\cos\theta = \frac{u_{s\alpha}(t)}{|\underline{u}_s(t)|} \quad (16)$$

### B. Estimation of unit vector

$i_{ms}$  makes an angle  $(\theta - 90^\circ)$  with the stator axis. Therefore, the  $\alpha, \beta$  components of  $i_{ms}$  can be written as follows:

$$i_{ms\alpha} = i_{ms} \sin\theta \quad (17)$$

$$i_{ms\beta} = -i_{ms} \cos\theta \quad (18)$$

We can write from (3)

$$i_{ra} = i_{ms\alpha} - (1 + \sigma_s) i_{s\alpha} \quad (19)$$

$$i_{r\beta} = i_{ms\beta} - (1 + \sigma_s) i_{s\beta} \quad (20)$$

$^s i_r$  can be calculated as:

$$^s i_r = \sqrt{i_{ra}^2 + i_{r\beta}^2} \quad (21)$$

The unit vectors for  $^s i_r$  (rotor current referred to stator) can be written as

$$\cos\rho_1 = \frac{i_{ra}}{|^s i_r|} \quad (22)$$

$$\sin\rho_1 = \frac{i_{r\beta}}{|^s i_r|} \quad (23)$$

Angle  $\rho_1$  is the angle between  $\underline{i}_r$  and stator axis as shown in Fig. 3.

The unit vectors for  $\underline{i}_r$  (rotor current) can be written as

$$\cos\rho_2 = \frac{i_{ra}}{|i_r|} \quad (24)$$

$$\sin\rho_2 = \frac{i_{rb}}{|i_r|} \quad (25)$$

Angle  $\rho_2$  is the angle between  $\underline{i}_r$  and rotor axis as shown in Fig. 3.

The unit vectors pertaining to the rotor position  $\epsilon = \rho_1 - \rho_2$  can be written as:

$$\sin \epsilon = \sin(\rho_1 - \rho_2) = \sin \rho_1 \cos \rho_2 - \cos \rho_1 \sin \rho_2 \quad (26)$$

$$\cos \epsilon = \cos(\rho_1 - \rho_2) = \cos \rho_1 \cos \rho_2 + \sin \rho_1 \sin \rho_2 \quad (27)$$

It may be noted here that the unit vectors  $\sin \epsilon$  and  $\cos \epsilon$  corresponding to the rotor position suffice for executing vector control algorithm. The actual value of  $\epsilon$  need not be computed through inverse function.

### C. Computation of $i_{ms}$

Stator flux can be calculated directly by stator voltage integration. Stator flux magnetizing current  $i_{ms}$  can be calculated from stator flux. However, in order to calculate  $i_{ms}$ , the magnetizing inductance  $L_0$  is required. If there is a substantial boost in the grid voltage or dip in the grid frequency,  $L_0$  is most likely to saturate. This will lead to incorrect calculation of  $i_{ms}$ .

$i_{ms}$  can be correctly estimated by adopting the following method of recomputation. Present rotor current sample is transformed to the stator coordinates using the unit vectors computed in the previous interval.

$$i_{r\alpha} = i_{ra} \cos \epsilon - i_{rb} \sin \epsilon \quad (28)$$

$$i_{r\beta} = i_{rb} \cos \epsilon + i_{ra} \sin \epsilon \quad (29)$$

$\alpha$  and  $\beta$  components of stator current  $i_{ms}$  can be written as:

$$i_{ms\alpha} = (1 + \sigma_s) i_{s\alpha} + i_{r\alpha} \quad (30)$$

$$i_{ms\beta} = (1 + \sigma_s) i_{s\beta} + i_{r\beta} \quad (31)$$

Magnitude of  $i_{ms}$  can be computed as:

$$|i_{ms}| = \sqrt{i_{ms\alpha}^2 + i_{ms\beta}^2} \quad (32)$$

### D. Estimation of speed

Speed of the machine is required for wind-energy conversion systems where the active power reference is made to vary as a function of the rotor speed to the possible maximum power. The speed of the machine can be estimated by using the following equation:

$$\omega_{est} = \cos \epsilon \frac{d}{dt} \sin \epsilon - \sin \epsilon \frac{d}{dt} \cos \epsilon \quad (33)$$

The usual method of speed calculation i.e. differentiation of rotor position ( $\omega_{est} = \frac{d}{dt} \epsilon$ ) would require  $\epsilon$  to be computed from the unit vectors using inverse trigonometric function. This is avoided in this method of speed estimation. Moreover  $\epsilon$  is discontinuous at  $\epsilon = 2\pi$ . But unit vectors are smoothly varying continuous functions and easier to differentiate without checking for discontinuity.

Per unit speed can be estimated as

$$\omega_{est} = [\cos \epsilon[k] (\sin \epsilon[k] - \sin \epsilon[k-1]) - \sin \epsilon[k] (\cos \epsilon[k] - \cos \epsilon[k-1])] / \frac{2\pi T_s}{T_b} \quad (34)$$

where  $T_s$  is the sampling period and  $T_b$  is the base period.

## III. SIMULATION RESULTS

PSCAD simulation software has been used to develop the experimental circuit of DFIG. Stator side is connected to 3-phase power supply or grid. Rotor side is connected to converter. The software is organised to work with time slot of 50 micro-seconds.

A comparison between the actual position unit vector ( $\sin \epsilon$ ) generated by the encoder with the position unit vector ( $\sin \epsilon$ ) computed employing the proposed sensorless method is given in Fig. 4 and Fig. 5. Fig. 4 is actual and estimated position during starting. Fig. 5 is actual and estimated position during torque transient. It is observed that estimated position has almost zero error. Similarly, a comparison between the actual speed generated by the encoder with the speed computed employing the proposed sensorless method is given in Fig. 6 and Fig. 7. Fig. 6 is actual and estimated speed during starting. Fig. 7 is actual and estimated speed during torque transient. It is observed that estimated position has almost zero error.

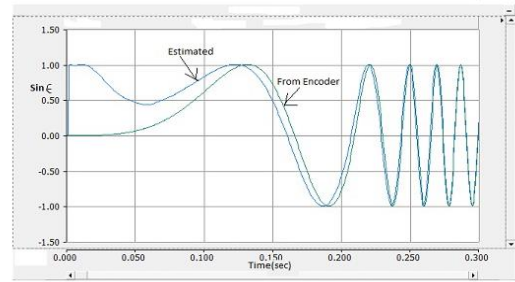


Fig. 4. Actual and estimated position during starting

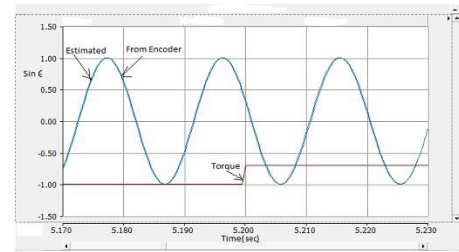


Fig. 5. Actual and estimated position during torque change

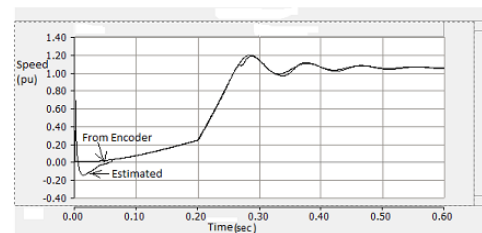


Fig. 6. Actual and estimated speed during starting

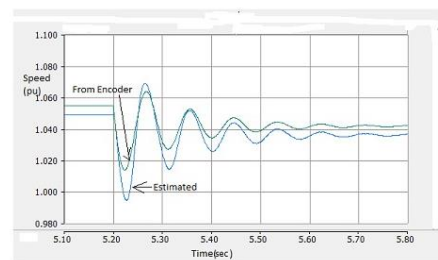


Fig. 7. Actual and estimated speed during torque change

Rating of the DFIG which is taken for simulation is as follows:

Voltage rating: 400 V  
kVA rating: 2 kVA  
Base angular frequency: 314.16 rad/s  
Angular moment of inertia: 0.1 s  
Stator resistance: 0.406 pu  
Rotor resistance: 0.0683 pu

## V. CONCLUSION

Mathematical model of DFIG has been derived. The model is simple as it directly follows the rotor voltage equations. Different parameters of DFIG are estimated and compared. Errors are negligible. If estimation is correct, then this can be applied to DFIG, and the encoder is not required to connect. If encoder is not connected in the machine, then system is simple and more economic. This machine model can be used in the simulation of a big power systems network.

### (1) REFERENCES

- [1] Raja P., Selvan M. P., Kumaresan N., "Enhancement of voltage stability margin in radial distribution system with squirrel cage induction generator based distributed generators", IET Generation, Transmission & Distribution, Vol. 7, No. 8, 2013, pp. 898-906
- [2] Datta R., Ranganathan V. T., "Direct power control of grid-connected wound rotor induction machine without rotor position sensors", May 2001, Vol. 16, no. 3, pp. 390-399
- [3] Zhang Y., Hu J., Zhu J., "Three-Vectors-Based Predictive Direct Power Control of the Doubly Fed Induction Generator for Wind Energy Applications", IEEE Transactions on Power Electronics, 2014, Vol. 29, Iss. 7, pp. 3485-3500
- [4] Datta R., Ranganathan V. T., "Decoupled control of active and reactive power for a grid-connected doubly-fed wound rotor induction machine without position sensors", IEEE Industry applications Conference, 3-7 Oct., 1999
- [5] Pena R., Clare J. C., Asher G. M., "Doubly fed induction generator using back-to-back PWM converters and its application to variable speed wind-energy generation", IEE Proceedings- Electric Power Applications, Vol. 143, No. 3, May 1996, pp. 231-241
- [6] Hazarika D., Das R., "Use of DFIG for Improvement of Voltage Stability Condition of a Power System", Journal of The Institution of Engineers (India): Series B, Vol. 99, Iss. 1, Feb. 2018, pp. 61-69
- [7] Djoudi A., Bacha S., Iman-Eini H., Rekioua T., "Sliding mode control of DFIG powers in the case of unknown flux and rotor currents with reduced switching frequency", International Journal of Electrical Power & Energy Systems, Vol. 96, March 2018, pp. 347-356
- [8] Wu F., Zhang X-P., Godfrey K. and Ju P. "Small signal stability analysis and optimal control of a wind turbine with doubly fed induction generator", IET Generation, Transmission, and Distribution, 2007, Vol. 1, Iss. 5, pp. 751-760
- [9] Abad G., Rodriguez M. A., Iwanski G., and Poza J. "Direct power control of doubly-fed-induction-generator-based wind turbines under unbalanced grid voltage", IEEE Transactions on Power Electronics, 2010, Vol. 25, Iss. 2, pp. 442-452

### (2) AUTHOR PROFILE



**Ranjay Das** is currently working as an Assistant Professor at Central Institute of Technology Kokrajhar BTR Assam India. He had more than ten years of teaching experience. His area of research is wind power generation, power system planning etc.